Published in final edited form as:
*Cancer Res*. 2012 March 15; 72(6): 1579–1587. doi:10.1158/0008-5472.CAN-11-2055.

# BMK1 kinase suppresses epithelial-mesenchymal transition through the Akt/GSK3β signaling pathway

**Runqiang Chen**[1,*], **Qingkai Yang**[1,*], and **Jiing-Dwan Lee**[1]

[1]Department of Immunology and Microbial Science, The Scripps Research Institute, 10550 North Torrey Pines Road, La Jolla, CA 92037, USA

## Abstract

Epithelial-mesenchymal transition (EMT) plays a crucial role in the development of cancer metastasis. The MAP kinases ERK, JNK and p38 have been implicated in promoting EMT, but a role for the MAP kinase BMK1 has not been studied. Here we report that BMK1 signaling suppresses EMT. BMK1 elevation augmented E-cadherin-mediated cell-cell adhesion, downregulated mesenchymal markers and decreased cell motility. Conversely, BMK1 silencing attenuated E-cadherin-mediated cell-cell adhesion, upregulated mesenchymal markers and stimulated cell motility. BMK1 depletion dramatically increased the accumulation of endogenous Snail in the nuclear compartment. Snail accumulation was mediated by Akt/GSK3β signaling, which was activated by a modulation in the expression of the mTOR inhibitor DEPTOR. In support of these observations, BMK1 depletion promoted metastasis in vivo. Together, our findings reveal a novel mechanism of EMT control via mTOR/Akt inhibition that suppresses cancer metastasis.

## Introduction

The process of epithelial-mesenchymal transition (EMT) is critically involved in the progression of human diseases, such as cancer metastasis and fibrosis (1). EMT involves profound phenotypic changes that include loss of cell-cell adhesion, loss of cell polarity, and acquisition of migratory and invasive properties (2). Loss of E-cadherin expression is a hallmark of EMT and has become an established biomarker of the process itself (3). One principal mechanism that acts to reduce E-cadherin expression in EMT is the activation of its associated transcriptional repressors. The E-cadherin repressors have been classified into two groups, based upon their interaction with the E-cadherin promoter (2). The first group directly binds to the E-cadherin promoter to physically inhibit transcription, and is composed of the Snail, Zeb, E47, and KLF8 factors (4, 5). The second group indirectly binds to the E-cadherin promoter, interacting with other direct binding factors, and includes Twist, Goosecoid, E2.2 and FoxC2. Gaining a thorough understanding of the process by which epithelial cells transit to mesenchymal cells is necessary for elucidating the molecular mechanisms that control cancer progression. The majority of mitogenic/oncogenic signal-activated signaling pathways stimulate EMT (2). In particular, three out of the four MAP kinase pathways described to date (namely, Erk, JNK and p38 (6)) induce EMT (7). The function of the fourth MAP kinase, BMK1, in EMT, however, remains unknown. Herein, we describe our investigations into the actions of BMK1 in EMT and in cancer metastasis.

Corresponding author: Jiing-Dwan Lee, Department of Immunology and Microbial Science, The Scripps Research Institute, 10550 N. Torrey Pines Rd., IMM12, La Jolla, California 92037, Fax: (858) 784-8343, Tel: (858) 784-8703, jdlee@scripps.edu.
*These authors contributed equally to this work.

## Materials and Methods

### Cell culture and reagents

The human cell lines A549, MCF10A, DU145, T47D and mouse cell line 4T1 were purchased from the American Type Culture Collection (ATCC) and cultured no more than 6 months after purchase for the experiments described herein. The cell lines were authenticated by ATCC and maintained as recommended. LY294002, U0126 and SB203580 were purchased from Calbiochem. Sanguinarine was purchased from Sigma-Aldrich.

### Plasmids, virus production and infection of target cells

The human plasmid pWZL-Neo-Myr-Flag-MAPK7, DEPTOR shRNA and DEPTOR cDNA were purchased from Addgene. The human shSnail plasmid was from Origene. The procedures used to produce retroviruses and to infect target cells have been described previously (8). To produce recombinant lentiviruses, vectors encoding shRNA against human BMK1, mouse BMK1 or control non-target shRNAs were purchased from Open Biosystems; lentiviruses were generated by co-transfection of subconfluent human embryonic kidney (HEK) 293FT cells (Invitrogen) with one of the above expression plasmids and a packaging plasmid (pMDL, pREV or pVSVG) using the GenJet DNA *in vitro* transfection reagent (SignaGen Laboratories). Infectious lentiviruses were collected 48 h after transfection and centrifuged to remove cell debris. A549 cells were transduced with the viruses expressing shRNA against human BMK1, DEPTOR, Snail or non-target shRNAs. 4T1 cells were transduced with lentiviruses expressing shRNA that targeted mouse BMK1 or non-target shRNAs.

### Antibodies and immunoblotting

Cells were lysed in RIPA buffer and blots were performed as described previously (9). Antibodies used were: anti-GAPDH (Sigma-Aldrich); anti-Snail, anti-GSK3β, anti-GSK3β (Ser 9), anti-Akt, anti-p-Akt (Ser 473), anti-p-BMK1 (T218/Y220), anti-p-Akt (Thr 308), anti-ZO-1 and anti-E-cadherin (Cell Signaling); anti-DEPTOR (Novus Biologicals); anti-Vimentin V9 (NeoMarkers); anti-N-cadherin (BD Transduction); anti-twist1, anti-Zeb1 and anti-Zeb2 (Santa Cruz Biotechnology); and anti-BMK1 (10). All immunoblotting experiments were repeated at least 3 times. The statistics for immunoblotting experiements in Figures 1–6 were presented in Supplementary Fig. S1 and S2 (Statistics for immunoblotting in Fig. 1C, 2B, 2E, 3A, 3B, 3C and 3G are in supplementary Fig. S1A, S1B, S1C, S1D, S1E, S1F and S1G, respectively. Statistics for immunoblotting in Fig. 3E, 3F, 4A, 4B, 4C, 4D, 4F, 5A and 5C are in supplementary Fig. S2A, S2B, S2C, S2D, S2E, S2F, S2G, S2H and S2I, respectively).

### Luciferase assay

The luciferase assay was performed as described previously (10). The pG5E1bLuc and internal control pRL-TK plasmids were cotransfected into cells along with a construct encoding the GAL4-binding domain fused to MEF2C.

### Immunoflourescence

Cells were grown on glass coverslips in a six-well plate and washed three times with PBS prior to fixing with 2% formaldehyde in PBS (pH7.4) for 15 min at room temperature. The cells were then washed three times with PBS and permeabilized with 0.2% Triton X-100 plus 1% normal goat serum (NGS) in PBS for five min on ice. Cells were again washed three times with 1% NGS in PBS. Coverslips were incubated with respective primary antibodies at 1:100 dilutions overnight at 4°C. After three washes with 1% NGS in PBS, incubation with fluorescein-conjugated secondary antibodies at 1:50 dilutions was carried

out. Cells were then washed four times with PBS, mounted with medium containing 4′,6-diamidino-2-phenylindole (DAPI; Vector Laboratories) and analyzed using fluorescence microscopy.

### Cell motility assays

Cells were harvested with Trypsin/EDTA, washed twice with DMEM, and resuspended in serum-free medium at a density of $10^6$ cells/ml. Lower chambers (Corning Life Sciences) were filled with 600 μl of complete medium, and the upper chambers were filled with 100 μl of the cell suspension. After four hrs of incubation at 37°C in 5% $CO_2$, the cells were fixed for 30 min at room temperature in 5% glutaraldehyde prepared in PBS. Staining was carried out for 30 min in 0.1% crystal violet and 2% ethanol. Non-migratory cells on the upper surface of the filter were removed by cotton swab. The number of migratory cells that had infiltrated the filter was measured by counting three random fields per filter. Mean values were obtained from at least three separate experiments.

### Wound healing assay

Cells were grown to confluence in a 6-well plate, and were wounded using a 1000-mL sterile pipette tip. The wounded area was photographed at 0 and 30 h. The distance traveled by cells at the migrating edge after 30 h was calculated by measuring three separate points within each field of view, from at least three separate experiments.

### Isolation of nucleus

Nucleus were prepared from cells using the protocol from previous study (11).

### Metastasis assay

Parental 4T1 or 4T1 breast cancer cells transduced with lentiviruses expressing shRNAs against mouse BMK1 or non-target shRNAs were harvested, counted and resuspended in PBS. Cells ($1\times10^5$ cells) were injected into the fat pad of the mammary gland of six to eight weeks old female BALB/c mice (The Scripps Research Institute). Primary tumors were dissected, weighed, and measured after 3 weeks. The number of lung metastasis was determined by counting the number of metastatic nodules on the lung surface. The lung tissues were fixed for standard hemotoxylin and eosin (H&E) staining.

### Statistical analyses

Results are presented as average ± SEM. The confidence level was calculated using Student’s t test. A P value of $<0.05$ was considered statistically significant.

## Results

Increased expression of BMK1 has been previously demonstrated to coincide with metastatic progression in a mouse mammary tumor model (12); however, the role of BMK1 in tumor metastasis remained unclear. Recently, EMT was shown to be positively correlated with metastatic potential of tumor cells (13, 14). Considering that the other three MAPK pathways are well-established promoters of EMT (6, 7, 15), we initially hypothesized that the BMK1 MAPK cascade would play a similar stimulatory role. To test this, we augmented the expression of BMK1 in tumor cells and were surprised to find that increased expression of BMK1 led to the development of close cell-cell contacts, which are morphological hallmarks of mesenchymal-epithelial transition (MET) (1) (Fig. 1A). We next investigated whether the molecular alterations of MET also occurred in these cells by examining the localization of several adherent junction proteins, including E-cadherin and ZO-1. Immunostaining of cells with enhanced BMK1 expression showed that all three adherent

junction proteins were significantly upregulated in the cell membrane, as compared to the levels detected in control cells (Fig. 1B). We also observed augmented expression of E-cadherin and ZO-1 proteins in the BMK1-upregulated cells by immunoblotting (Fig. 1C). In contrast, the expression of mesenchymal markers, Vimentin and N-cadherin, appeared to be downregulated (Fig. 1B and C). Moreover, we found that the transactivation activity of MEF2C, a direct substrate of BMK1 (10), is upregulated (Fig. 1D) and the phosphorylation of the activating loop of BMK1 is augmented in BMK1 cells in comparison with that in EV cells (Supplementary Fig. S3A). These results suggest that the activity of BMK1 is increased in BMK1 A549 cells. As MET is known to inhibit cell migration, we found that, indeed, BMK1-upregulated cells exhibited significantly slower serum-induced directional migration, as compared to that of control cells (Fig. 1E). However, increased expression of BMK1 didn't affect the cell proliferation (Supplementary Fig. S3B), apoptosis (Supplementary Fig. 3C) and *in vitro* tumorigenicity (Supplementary Fig. S3D). Hence, our results indicated that upregulation of BMK1 enhanced the epithelial properties of cells.

Conversely, to examine whether reduced expression of BMK1 in tumor cells would have the opposite effect, we knocked-down BMK1 in tumor cells and found that BMK1 deficiency resulted in loss of cell-cell contacts and obvious cell scattering, both of which are morphological hallmarks of EMT (1) (Fig. 2A). By immunoblotting, we also observed substantial reduction in the levels of E-cadherin and ZO-1 proteins in response to BMK1-depletion (Fig. 2B). As expected, the expression of the mesenchymal markers, Vimentin and N-cadherin, was upregulated (Fig. 2B). Moreover, using transwell migration and wound healing assays, we found that BMK1-depleted cells appeared to migrate faster than control cells (Fig. 2C and D). To investigate whether BMK1 depletion can also promote EMT in other cell lines, we created shBMK1 stable cell lines in human prostate cancer cell (DU145) and non-tumorigenic epithelial cell (MCF10A). We found that BMK1 knockdown not only reduced the expression levels of epithelial markers, E-cadherin and ZO-1 proteins, upregulated those of mesenchymal markers, N-cadherin and Vimentin proteins, but also increased cell migration in both MCF10A and DU145 cells, as compared to control cells (Fig. 2E). Taken together, these results indicated that the BMK1 pathway acts as a critical cellular brake for EMT and metastasis (Fig. 2F), a surprising mechanism as most of the mitogenic/oncogenic signaling pathways are known to trigger EMT.

To identify the downstream molecules involved in EMT and modulated by BMK1 pathway activity, we analyzed the expression levels of several known E-cadherin transcriptional repressors in BMK1-depleted cells. The expression level of Snail was found to be the only protein significantly upregulated in BMK1-depleted cells, as compared to levels in control cells (Fig. 3A). In contrast, the expression level of Snail was downregulated in BMK1-upregulated cells, as compared to levels detected in control cells (Fig. 3A). Interestingly, the expression level of Snail mRNA transcripts did not change in response to altered BMK1 expression level (data not shown). As the Snail protein is known to be destabilized after translocation out of the nucleus, following its phosphorylation by GSK3β (16, 17), we first tested whether BMK1 was involved in the Snail translocation event. We found that Snail protein was dramatically increased in the nuclear compartments of BMK1-depleted cells, as compared to that of control cells (Fig. 3B). In addition, we knockdown Snail in BMK1-deficient cells and discovered that depletion of Snail in shBMK1 cells inhibited about 50% of EMT induced by BMK1 reduction (Supplementary Fig. S4A). This result indicates the augmentation of Snail protein level is one of the major causes for BMK1 depletion-induced EMT. As Snail silencing only block EMT caused by BMK1-reduction by about 50%, additional EMT regulator(s) other than Snail may also notably contribute to the BMK1-dependent phenomemon. Next, we tested whether the stabilization of Snail by BMK1 depletion was mediated through modulation of the GSK3β activity. We found that GSK3β phosphorylation (at Serine 9) was significantly increased in BMK1-deficient cells and

decreased in BMK1-overexpression cells, as compared to control cells (Fig. 3C). Since loss of phosphorylation at S9 is known to enhance GSK3β activity (18), our results indicated that BMK1 depletion-mediated Snail stabilization is dependent on the deactivation of GSK3β via phosphorylation.

As GSK3β activity can be regulated by the PI3K, ERK1/2 and p38 pathways (19), and the association of Snail with GSK3β can be inhibited by the NF-κB pathway (18), we sought to determine which particular signaling pathway is involved in BMK1 depletion-induced Snail stabilization. To this end, we treated BMK1-depleted cells with inhibitors specific to each of these signaling pathways and discovered that the stabilization of Snail related to BMK1 depletion was only notably inhibited by the PI3K inhibitor (LY294002) (Fig. 3D and E). This finding suggested that the PI3K pathway is critical for BMK1 depletion-induced Snail stabilization. In support of this notion, we also found that the activity of Akt, a downstream effector of PI3K, was upregulated in BMK1-depleted cells, as compared to control cells (Fig. 3F). Moreover, LY294002 treatment only had marginal effect on BMK1 activity (Supplementary Fig. S4B) and U0126 treatment only slightly upregulated the expression level of Snail in cells (Supplementary Fig. S4C). Collectively, these results suggested that BMK1 promotes Snail degradation through suppression of the PI3K/Akt pathway.

Akt regulates cell proliferation, growth, survival, and metabolism (20). Full activation of Akt requires phosphorylation of S473 in the hydrophobic motif by mTOR complex 2 (mTORC2) (21–23), as well as phosphorylation of T308 in the activation loop by PDK1, a downstream effector of PI3K (20, 24–26). To further investigate which molecule was primarily responsible for regulating BMK1-dependent suppression of the PI3K/Akt pathway, gene expression profiles between BMK1-depleted cells and control cells were analyzed (data not shown). We found that the expression level of DEPTOR transcripts was decreased in BMK1-depleted cells. DEPTOR is an mTOR inhibitor in cancer cells (27) and exists in two functionally distinct complexes, mTORC1 and mTORC2 (28–31). Depletion of cellular DEPTOR increases not only the phosphorylation of S473 (27) but also that of T308 of AKT (personal communication with Dr. Peterson). Hence, we examined the expression level of DEPTOR in BMK1-depleted tumor cells and found that DEPTOR protein was significantly decreased, as compared to that of control cells (Fig. 4A). Next, we tested whether decreased DEPTOR expression was able to induce EMT. Indeed, the depletion of DEPTOR was associated with reduced expression of the epithelial marker E-cadherin and with increased expression of the mesenchymal marker N-cadherin (Fig. 4B). As expected, depletion of DEPTOR increased the phosphorylation of both S473 and T308 in AKT (Fig. 4B), similar to what we observed in BMK1-depleted cells.

BMK1 activity was only marginal upregulated by DEPTOR knockdown (Supplementary Fig. S4D). Moreover, we found that Snail protein was significantly increased in the nuclear compartments of DEPTOR-depleted cells, as compared to that of control cells (Fig. 4C). These results indicated that DEPTOR depletion can induce EMT in cancer cells. To examine the contribution of DEPTOR in EMT induced by BMK1 knockdown, we amplified the expression level of DEPTOR in BMK1-deficient cells. The increased cellular DEPTOR levels coincided with increased ability of BMK1 depletion to induce expression of mesenchymal markers and to significantly diminish that of epithelial markers (Fig. 4D). These results indicated that DEPTOR plays a critical role in EMT regulation by BMK1 (Fig. 4E). Moreover, we tested three other BMK1 pathways (BMK1-MEF2C(10), BMK1-SGK (32) and BMK1-PML (33) for their involvement in EMT by expressing MEF2C or SGK mutants that can block BMK1-mediated activation of these two molecules in cells as well as by knocking down PML expression in cells (Supplementary Fig. S4E, F and G). We found that expression of MEF2C mutant and knocking down PML have no effect in E-Cadherin expression but the expression of SGK mutant somewhat reduced the expression level of E-

Cadherin (Supplementary Fig. S4E, F and G). This data indicates that other than BMK1-DEPTOR pathway, BMK1-SGK pathway may also have a minor role in EMT induced by BMK1 depletion. We also compared the mRNA levels of four MAPKs, BMK1, ERK1, p38 and JNK1 in cancer cells (Fig. S4H). We found that the message levels of BMK1 and ERK1 are higher than p38 and JNK1. As both BMK1 and ERK1 contribute to cell proliferation/survival, cancer cells may selectively increase the message of these two MAPKs to help driving the uncontrolled growth of tumor. As translational and post-translational modulation of these kinases also contribute to the final cellular protein concentrations of these kinases, the eventual protein expression levels may vary from the message levels of these kinases.

Augmented Akt signaling has been characterized in several cancer cells as being associated with inactivating PTEN mutations and activating PIK3CA mutations (34). To investigate whether BMK1 can also suppress EMT in cancer cell lines with constitutive Akt signaling, we created shBMK1 stable cancer cell lines from PIK3CA mutation cell line with high p-Akt (T47D) and wild-type cells with normal profiles of PIK3CA (DU145). We found that BMK1 knockdown not only downregulated DEPTOR protein expression levels but also activated AKT and reduced E-cadherin protein expression in DU145 cell (Fig. 4F). Although BMK1 knockdown also reduced the DEPTOR protein expression in T47D cell with constitutive Akt signaling, the phosphorylation states of AKT and E-cadherin protein expression levels were not significantly affected (Fig. 4F). These data lent further support to our finding that BMK1 induces MET through the DEPTOR/Akt/GSK3β signaling module.

As EMT is a critical regulator of cancer metastasis (35), and BMK1 depletion promotes EMT in cancer cells, we investigated whether reduction of cellular BMK1 levels would increase the metastatic potential of carcinoma cells. To this end, we generated a BMK1-depleted tumor cell line, with endogenous BMK1 reduced by >75% (Fig. 5A). We also observed the reduction in the level of epithelial marker, E-cadherin protein and the increase in that of the mesenchymal marker, Vimentin protein in BMK1-depleted cells, as compared to these markers' levels detected in control cells (Fig. 5A). These cells were then transplanted into the mammary fat pad of mice; three weeks later, the weight of tumors from mice transplanted with BMK1-depleted cells was slightly decreased compared with controls (Fig. 5B). The numbers of metastatic nodules on the surface of the lungs were significantly higher in those mice injected with BMK1-depleted tumor cells than in those injected with control cells (Fig. 5C and D). Moreover, in lung tumor tissues, we also detected the decreasing expression level of E-cadherin protein as well as the increasing level of Vimentin protein in BMK1-depleted tumor tissues in comparison with that of control tumor tissues (Fig. 5E). We also tested the effect of increased expression of BMK1 on the metastatic potential of 4T1 cell. We found that increased BMK1 expression (Supplementary Fig. S5A) has little or no effect on the weight of implanted primary tumor (Supplementary Fig. S5B) but that increased BMK1 level considerably suppresses the metastatic potential of 4T1 cells (Supplementary Fig. S5C and S5D). These data suggested that when BMK1 was reduced in tumor cells the metastasis rate of carcinoma cells was enhanced.

## Discussion

EMT is a pivotal cellular process for proper development and for cancer metastasis. EMT is triggered by mitogens, such as TGF-β and FGF families, EGF and SF/HGF (13, 36). The intracellular signaling mediators activated by such mitogens were also implicated in positive regulation of the EMT process. These particular intracellular signaling molecules include members of the receptor tyrosine kinase (RTK) family (37), the small GTPase family and the MAPK family (13). To date, four distinct MAPK signaling cascades have been identified in mammals, three of which, Erk, JNK and p38, are known to promote EMT by downregulating E-cadherin through distinct mechanisms (6, 7, 15, 38). The fourth pathway,

BMK1, is less well characterized as it is the most recently discovered and least studied. Surprisingly, we discovered that BMK1 acts to suppress EMT through a mechanism involving increasing the expression of E-cadherin. Furthermore, using 4T1 mouse breast cancer cells, we found that BMK1 may have a role in suppressing cancer metastasis. However, additional *in vivo* experiments in different metastasis models are needed to further clarify BMK1's role in metastasis in different cancer types and various stages of tumor development. However, our findings suggest that during cell activation by mitogens/oncogenic signals, the mitogens-activated BMK1 pathway acts as a critical cellular brake for EMT and cancer metastasis in order to antagonize most other mitogens-activated intracellular signaling cascades and to maintain appropriate cellular responses under numerous physiological and pathological conditions (Fig. 2F).

The stability of Snail is regulated by GSK3β (16) and NF-κB (18). Herein, we found that BMK1 regulates Snail stability through activating GSK3β, not NF-κB pathway (Fig. 3). Furthermore, we discovered that BMK1 activates GSK3β to destabilize Snail via suppressing the PI3K/Akt pathway. The PI3K/Akt pathway is not only a critical suppressor for GSK3β but also a major cellular survival signaling cascade involved in numerous developmental, physiological and pathological processes (20). In addition to EMT, GSK3β has also been implicated in the control of cellular response to damaged DNA and in regulating effectors in the Wnt and the Hedgehog pathways (39). Our finding that BMK1 negatively regulates PI3K/Akt activity, and consequently promotes GSK3β activity, suggests that the BMK1 pathway may also contribute to the various functions/phenotypes modulated by PI3K/Akt and GSK3β. In our case, the effect of BMK1 on EMT through regulating the PI3K/Akt/GSK3β signaling module is very significant. Nonetheless, the impact of the BMK1 pathway on the other PI3K/Akt- and/or GSK3β-dependent functions/phenotypes will need to be carefully evaluated. In addition, our finding of the ability of BMK1 to suppress PI3K/mTORC2/Akt pathway through regulating DEPTOR expression establishes the connection between the BMK1 pathway and the PI3K/Akt cascade.

Cancer metastasis is responsible for 90% of mortality experienced by solid cancer patients. Targeted blockade of receptor tyrosine kinases (RTKs) represents a popular new anti-cancer strategy to hinder tumor growth. Many RTK inhibitors have been clinically validated as having effective anti-cancer properties; these include iressa and tarceva (EGFR inhibitors), sorafenib and sunitinib (VEGFR inhibitors), and trastuzumab (HER2 inhibitor). However, increased metastasis has recently been observed in patients or experimental mice after sustained exposure to these RTK inhibitors (40, 41). Since these RTKs lie upstream of BMK1 and positively regulate its activity, deactivation of these RTKs during cancer treatment would be expected to suppress the BMK1 activity and, consequently, enhance cancer metastasis. As such, a combination of RTK and mTOR inhibitors should be able to abrogate this undesirable metastasis-promoting side effect of suppressing BMK1 activity during cancer therapies targeting RTKs.

In conclusion, our study to characterize the function of BMK1 in EMT led to the unexpected, and important, discovery that BMK1 signaling acts as an intrinsic brake for EMT and for cancer metastasis in cancer cells by antagonizing the other mitogenic/oncogenic signal-activated pathways (Fig. 2F). BMK1 was determined to suppress EMT and cancer metastasis through destabilization of a critical short-lived transcriptional factor, Snail, by the DEPTOR/PI3K/mTORC2/Akt/GSK3β signaling module. Depletion of cellular BMK1 caused a dramatic increase and accumulation of endogenous Snail in the nuclear compartment. Since endogenous Snail rarely reaches detectable levels in the nucleus, this finding suggests that BMK1 is a major modulator of Snail stability and EMT. Our findings not only revealed a novel BMK1-mediated mechanism for inhibiting the mTOR/Akt

signaling module and suppressing cancer metastasis but also provide important implications for developing effective treatment strategies for metastatic cancers.

## Supplementary Material

Refer to Web version on PubMed Central for supplementary material.

## Acknowledgments

This work was supported by grants from the NIH, CA079871 and CA114059, (to J.-D.L) and by funds from the Tobacco-Related Disease, Research Program of the University of California, 19XT-0084, (to J.-D.L.).

We thank Dr. Debbie Liao and Dr. Ralf Reisfeld for their help in establishing metastasis model.

## References

1. Acloque H, Adams MS, Fishwick K, Bronner-Fraser M, Nieto MA. Epithelial-mesenchymal transitions: the importance of changing cell state in development and disease. The Journal of clinical investigation. 2009; 119:1438–49. [PubMed: 19487820]
2. Thiery JP, Acloque H, Huang RY, Nieto MA. Epithelial-mesenchymal transitions in development and disease. Cell. 2009; 139:871–90. [PubMed: 19945376]
3. Kang Y, Massague J. Epithelial-mesenchymal transitions: twist in development and metastasis. Cell. 2004; 118:277–9. [PubMed: 15294153]
4. Peinado H, Olmeda D, Cano A. Snail, Zeb and bHLH factors in tumour progression: an alliance against the epithelial phenotype? Nature reviews Cancer. 2007; 7:415–28.
5. Wang X, Zheng M, Liu G, Xia W, McKeown-Longo PJ, Hung MC, et al. Kruppel-like factor 8 induces epithelial to mesenchymal transition and epithelial cell invasion. Cancer Res. 2007; 67:7184–93. [PubMed: 17671186]
6. Zohn IE, Li Y, Skolnik EY, Anderson KV, Han J, Niswander L. p38 and a p38-interacting protein are critical for downregulation of E-cadherin during mouse gastrulation. Cell. 2006; 125:957–69. [PubMed: 16751104]
7. Shin S, Dimitri CA, Yoon SO, Dowdle W, Blenis J. ERK2 but not ERK1 induces epithelial-to-mesenchymal transformation via DEF motif-dependent signaling events. Molecular cell. 2010; 38:114–27. [PubMed: 20385094]
8. Boehm JS, Zhao JJ, Yao J, Kim SY, Firestein R, Dunn IF, et al. Integrative genomic approaches identify IKBKE as a breast cancer oncogene. Cell. 2007; 129:1065–79. [PubMed: 17574021]
9. Chen RQ, Yang QK, Chen YL, Oliveira VA, Dalton WS, Fearns C, et al. Kinome siRNA screen identifies SMG-1 as a negative regulator of hypoxia-inducible factor-1alpha in hypoxia. The Journal of biological chemistry. 2009; 284:16752–8. [PubMed: 19406746]
10. Kato Y, Kravchenko VV, Tapping RI, Han J, Ulevitch RJ, Lee JD. BMK1/ERK5 regulates serum-induced early gene expression through transcription factor MEF2C. The EMBO journal. 1997; 16:7054–66. [PubMed: 9384584]
11. Andersen JS, Lyon CE, Fox AH, Leung AK, Lam YW, Steen H, et al. Directed proteomic analysis of the human nucleolus. Current biology: CB. 2002; 12:1–11. [PubMed: 11790298]
12. Yang J, Mani SA, Donaher JL, Ramaswamy S, Itzykson RA, Come C, et al. Twist, a master regulator of morphogenesis, plays an essential role in tumor metastasis. Cell. 2004; 117:927–39. [PubMed: 15210113]
13. Thiery JP, Sleeman JP. Complex networks orchestrate epithelial-mesenchymal transitions. Nature reviews Molecular cell biology. 2006; 7:131–42.
14. Kalluri R, Weinberg RA. The basics of epithelial-mesenchymal transition. The Journal of clinical investigation. 2009; 119:1420–8. [PubMed: 19487818]
15. Alcorn JF, Guala AS, van der Velden J, McElhinney B, Irvin CG, Davis RJ, et al. Jun N-terminal kinase 1 regulates epithelial-to-mesenchymal transition induced by TGF-beta1. Journal of cell science. 2008; 121:1036–45. [PubMed: 18334556]

16. Zhou BP, Deng J, Xia W, Xu J, Li YM, Gunduz M, et al. Dual regulation of Snail by GSK-3beta-mediated phosphorylation in control of epithelial-mesenchymal transition. Nature cell biology. 2004; 6:931–40.
17. Yook JI, Li XY, Ota I, Fearon ER, Weiss SJ. Wnt-dependent regulation of the E-cadherin repressor snail. The Journal of biological chemistry. 2005; 280:11740–8. [PubMed: 15647282]
18. Wu Y, Deng J, Rychahou PG, Qiu S, Evers BM, Zhou BP. Stabilization of snail by NF-kappaB is required for inflammation-induced cell migration and invasion. Cancer cell. 2009; 15:416–28. [PubMed: 19411070]
19. Cohen P, Frame S. The renaissance of GSK3. Nature reviews Molecular cell biology. 2001; 2:769–76.
20. Manning BD, Cantley LC. AKT/PKB signaling: navigating downstream. Cell. 2007; 129:1261–74. [PubMed: 17604717]
21. Sarbassov DD, Guertin DA, Ali SM, Sabatini DM. Phosphorylation and regulation of Akt/PKB by the rictor-mTOR complex. Science. 2005; 307:1098–101. [PubMed: 15718470]
22. Guertin DA, Stevens DM, Thoreen CC, Burds AA, Kalaany NY, Moffat J, et al. Ablation in mice of the mTORC components raptor, rictor, or mLST8 reveals that mTORC2 is required for signaling to Akt-FOXO and PKCalpha, but not S6K1. Developmental cell. 2006; 11:859–71. [PubMed: 17141160]
23. Jacinto E, Facchinetti V, Liu D, Soto N, Wei S, Jung SY, et al. SIN1/MIP1 maintains rictor-mTOR complex integrity and regulates Akt phosphorylation and substrate specificity. Cell. 2006; 127:125–37. [PubMed: 16962653]
24. Laplante M, Sabatini DM. mTOR signaling at a glance. Journal of cell science. 2009; 122:3589–94. [PubMed: 19812304]
25. Alessi DR, Pearce LR, Garcia-Martinez JM. New insights into mTOR signaling: mTORC2 and beyond. Science signaling. 2009; 2:pe27. [PubMed: 19383978]
26. Foster KG, Fingar DC. Mammalian target of rapamycin (mTOR): conducting the cellular signaling symphony. The Journal of biological chemistry. 2010; 285:14071–7. [PubMed: 20231296]
27. Peterson TR, Laplante M, Thoreen CC, Sancak Y, Kang SA, Kuehl WM, et al. DEPTOR is an mTOR inhibitor frequently overexpressed in multiple myeloma cells and required for their survival. Cell. 2009; 137:873–86. [PubMed: 19446321]
28. Bhaskar PT, Hay N. The two TORCs and Akt. Developmental cell. 2007; 12:487–502. [PubMed: 17419990]
29. Jacinto E, Lorberg A. TOR regulation of AGC kinases in yeast and mammals. The Biochemical journal. 2008; 410:19–37. [PubMed: 18215152]
30. Guertin DA, Sabatini DM. Defining the role of mTOR in cancer. Cancer cell. 2007; 12:9–22. [PubMed: 17613433]
31. Sengupta S, Peterson TR, Sabatini DM. Regulation of the mTOR complex 1 pathway by nutrients, growth factors, and stress. Molecular cell. 2010; 40:310–22. [PubMed: 20965424]
32. Hayashi M, Tapping RI, Chao TH, Lo JF, King CC, Yang Y, et al. BMK1 mediates growth factor-induced cell proliferation through direct cellular activation of serum and glucocorticoid-inducible kinase. The Journal of biological chemistry. 2001; 276:8631–4. [PubMed: 11254654]
33. Yang Q, Deng X, Lu B, Cameron M, Fearns C, Patricelli MP, et al. Pharmacological inhibition of BMK1 suppresses tumor growth through promyelocytic leukemia protein. Cancer cell. 2010; 18:258–67. [PubMed: 20832753]
34. Kang S, Bader AG, Vogt PK. Phosphatidylinositol 3-kinase mutations identified in human cancer are oncogenic. Proceedings of the National Academy of Sciences of the United States of America. 2005; 102:802–7. [PubMed: 15647370]
35. Thiery JP. Epithelial-mesenchymal transitions in tumour progression. Nature reviews Cancer. 2002; 2:442–54.
36. Yang J, Weinberg RA. Epithelial-mesenchymal transition: at the crossroads of development and tumor metastasis. Developmental cell. 2008; 14:818–29. [PubMed: 18539112]
37. Polyak K, Weinberg RA. Transitions between epithelial and mesenchymal states: acquisition of malignant and stem cell traits. Nature reviews Cancer. 2009; 9:265–73.

38. Bakin AV, Rinehart C, Tomlinson AK, Arteaga CL. p38 mitogen-activated protein kinase is required for TGFbeta-mediated fibroblastic transdifferentiation and cell migration. J Cell Sci. 2002; 115:3193–206. [PubMed: 12118074]

39. Doble BW, Woodgett JR. GSK-3: tricks of the trade for a multi-tasking kinase. J Cell Sci. 2003; 116:1175–86. [PubMed: 12615961]

40. Ebos JM, Lee CR, Cruz-Munoz W, Bjarnason GA, Christensen JG, Kerbel RS. Accelerated metastasis after short-term treatment with a potent inhibitor of tumor angiogenesis. Cancer cell. 2009; 15:232–9. [PubMed: 19249681]

41. Paez-Ribes M, Allen E, Hudock J, Takeda T, Okuyama H, Vinals F, et al. Antiangiogenic therapy elicits malignant progression of tumors to increased local invasion and distant metastasis. Cancer cell. 2009; 15:220–31. [PubMed: 19249680]

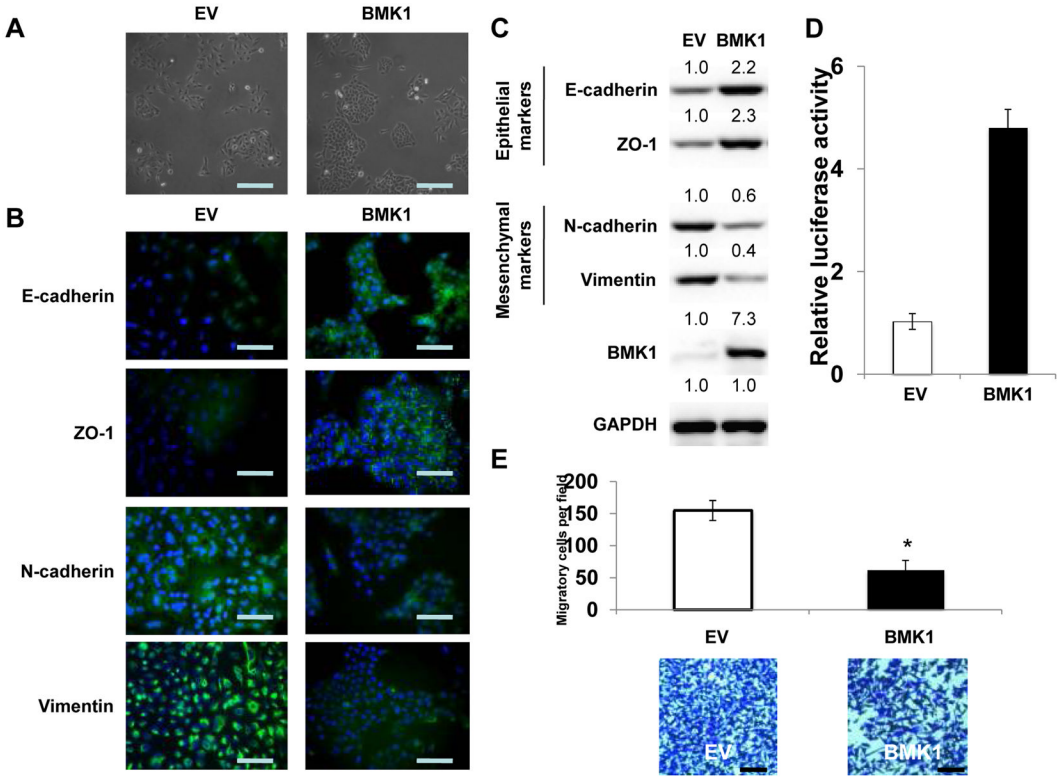


**Figure 1.**

BMK1 enhances cell epithelial properties

(A) Phase-contrast microscopic images of A549 cells carrying control vector (EV) or expression vector encoding BMK1. Scale bar represents 50 μm. (B) Fluorescence microscopic staining of E-cadherin, ZO-1, N-cadherin and Vimentin (green) is indicated in the EV and BMK1 A549 cells. Nuclear DNA was stained with DAPI (blue). Scale bar represents 20 μm. (C) Expression levels of epithelial markers, E-cadherin and ZO-1, as well as mesenchymal markers, N-cadherin and Vimentin, were examined by immunoblotting of EV and BMK1 A549 cells. GAPDH was used as a loading control. The relative expression levels of indicated proteins in BMK1 cells was determined by setting the expression level, measuring by densitometry, in EV cells at a value of 1.0. (D) MEF2C transactivation activity was determined in EV and BMK1 A549 cells using luciferase assay. (E) Motility of EV and BMK1 A549 cells was analyzed. Each bar represents the mean ± standard deviation (s.d.) of samples measured in triplicate. *, $P < 0.05$. Scale bar represents 50 μm.

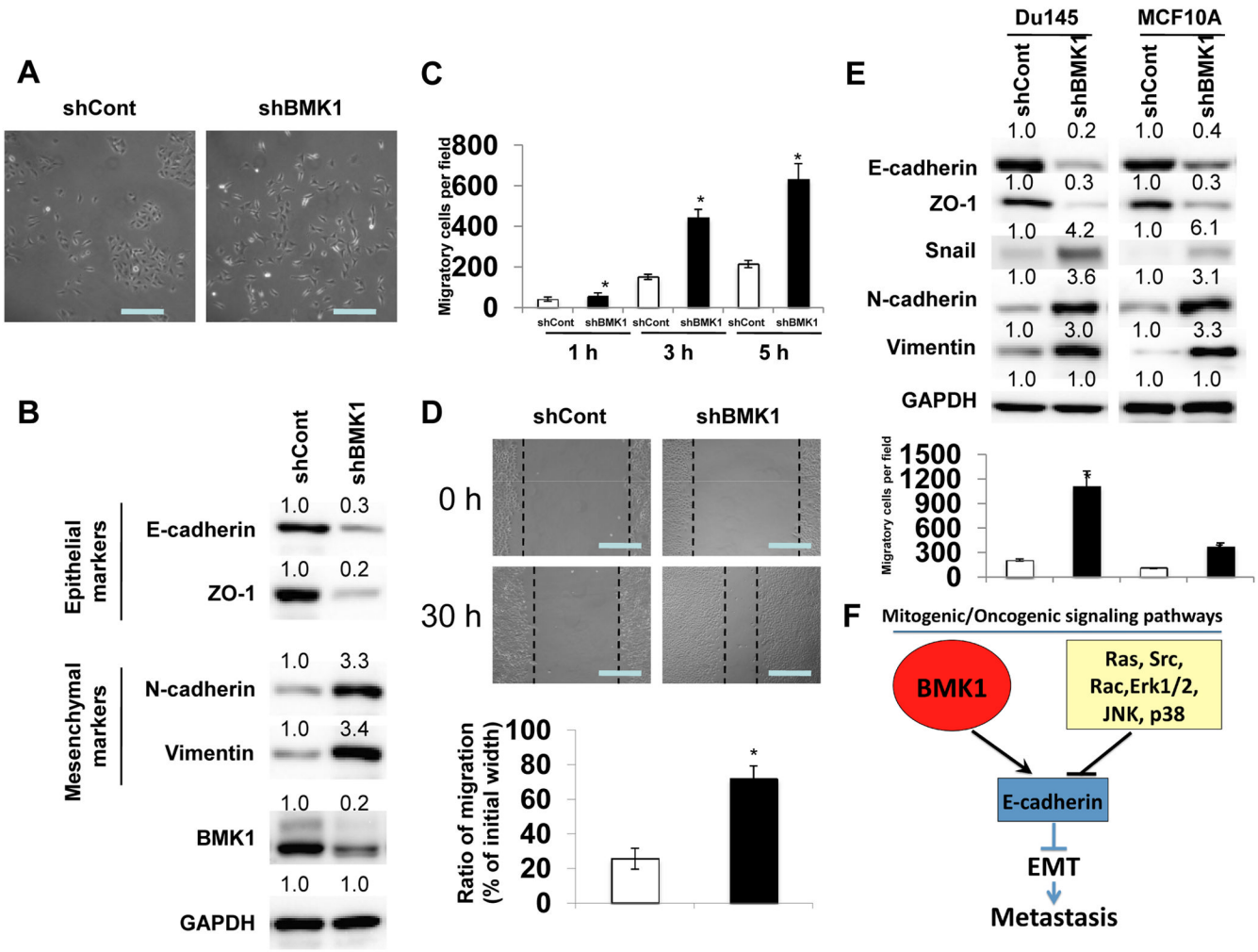


**Figure 2.**

BMK1 depletion induces EMT

(A) Phase-contrast microscopic images of A549 cells infected with lentiviral control shRNA (shCont) or shRNA vector targeting BMK1 (shBMK1). Scale bar represents 50 μm. (B) Expression levels of epithelial markers, E-cadherin and ZO-1, as well as mesenchymal markers, N-cadherin and Vimentin, were examined by immunoblotting in shCont and shBMK1 A549 cells. Protein level quantification was determined as in Fig. 1C by setting protein expression level in shCont cells at 1.0. (C) Motility of shCont and shBMK1 A549 cells was analyzed for indicated times. Each bar represents the mean ± s.d. of samples measured in triplicate. *, $P < 0.05$ (D) Migration of shCont and shBMK1 A549 cells in wound healing assays (pictures taken after 30 hr). Quantification was carried out by measuring the distance migrated compared with the controls from six separate assays and three separate measurements per assay. *, $P < 0.05$. Scale bar represents 50 μm. (E) Expression levels of E-cadherin, ZO-1, Snail, N-cadherin and Vimentin in DU145 and MCF10A cells were examined by immunoblotting. The motility was analyzed as in (C). (F) Proposed model of BMK1 antagonism of other mitogenic/oncogenic signaling pathways in EMT and metastasis.

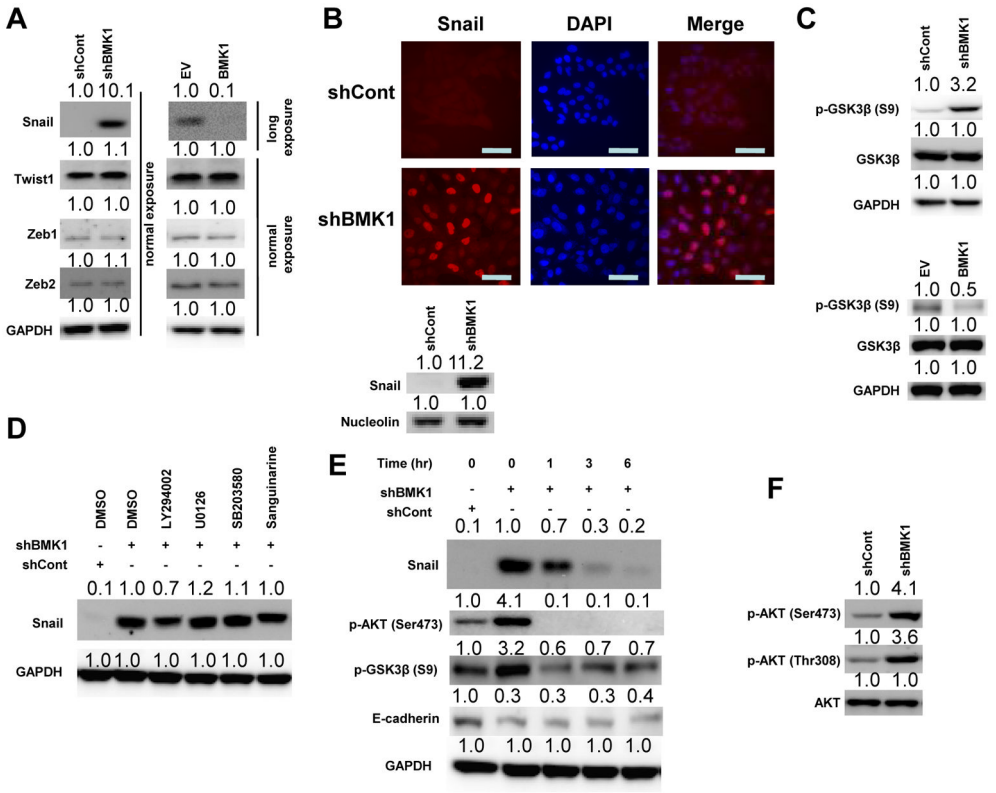


**Figure 3.**

BMK1 destabilizes Snail via the Akt/GSK3β signaling pathway

(A) Expression levels of transcription factors Snail, Twist1, Zeb1 and Zeb2 in shCont, shBMK1, EV and BMK1 A549 cells were detected by immunoblotting. Protein level quantification was determined by setting protein expression level in shCont or EV cells at 1.0. (Long exposure was used to collect Western Blot image for Snail protein in EV and BMK1 cells as indicated). (B) Fluorescent microscopic visualization of Snail (red) in the shCont and shBMK1 A549 cells. Nuclear DNA was stained with DAPI (blue). Scale bar represents 20 μm. Nuclear expression level of Snail was also examined by immunoblotting. (C) The activity of GSK3β in shCont, shBMK1, EV and BMK1 A549 cells was detected by immunoblotting using anti-p-GSK3β (Ser 9) antibody. Protein expression level in shCont cells was set at 1.0. (D) shBMK1 A549 cells were pretreated with various inhibitors (LY294002 [20 μM], UO126 [20 μM], SB203508 [20 μM] and Sanguinarine [1 μM]) for 1 hr. The level of Snail detected by immunoblotting is shown. Protein expression level in shCont cells was set at 1.0. (E) shBMK1 A549 cells were pretreated with LY294002 for various time points (as noted). The levels of Snail, p-AKT (Ser473), p-GSK3 β (S9) and E-cadherin detected by immunoblotting is shown. Protein expression level in shCont cells was set at 1.0. (F) Phosphorylation states and expression levels of Akt in shCont and shBMK1 A549 cells were examined by immunoblotting. Protein expression level in shCont cells was set at 1.0.

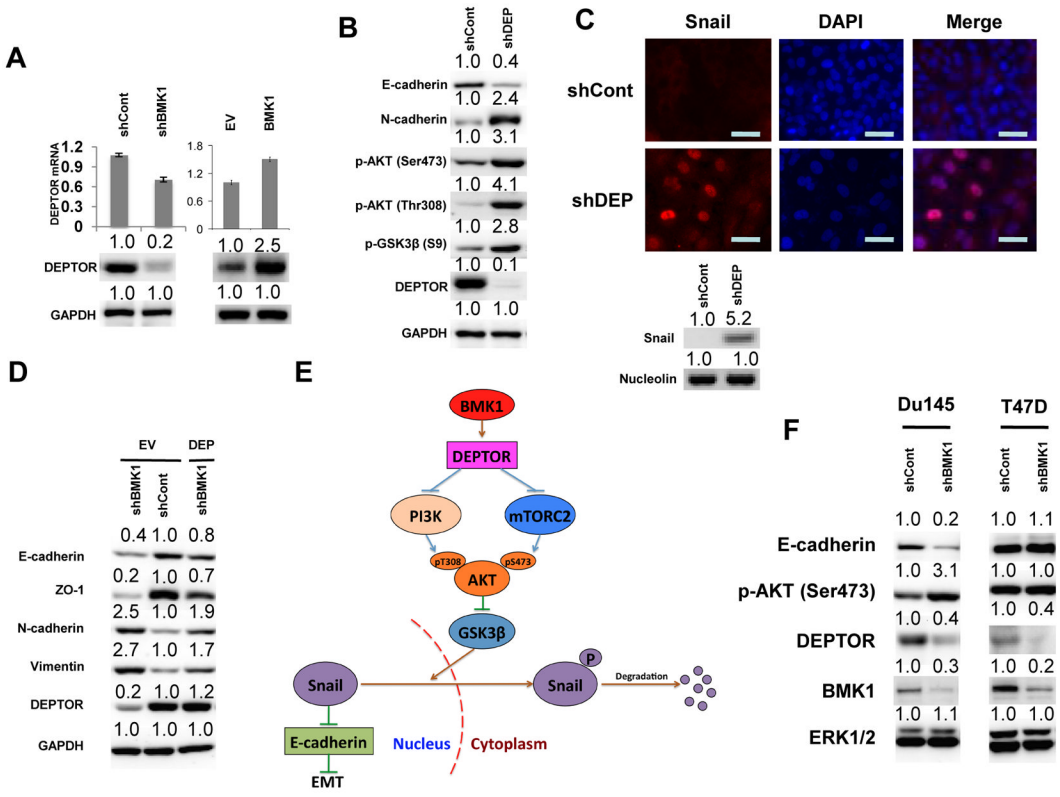


**Figure 4.**

BMK1 suppresses AKT/GSK3β/Snail pathway via DEPTOR

(A) The expression levels of DEPTOR in shCont, shBMK1, EV and BMK1 A549 cells were examined by immunoblotting. DEPTOR mRNA was measured by qRT-PCR, and normalized to GAPDH mRNA levels. Error bars indicate s.d. for three independent experiments. Protein expression level in shCont cells was set at 1.0. (B) Expression levels of E-cadherin, N-cadherin, and DEPTOR, as well as the phosphorylation states of Akt and GSK3β (S9), in shCont and shDEPTOR (shDEP) A549 cells were examined by immunoblotting. Protein expression level in shCont cells was set at 1.0. (C) Fluorescent microscopic visualization of Snail (red) in shCont and shDEP A549 cells. Nuclear DNA was stained with DAPI (blue). Scale bar represents 20 μm. Nuclear expression level of Snail was also examined by immunoblotting. (D) Expression levels of epithelial markers, E-cadherin and ZO-1, as well as mesenchymal markers, N-cadherin and Vimentin, and DEPTOR were examined by immunoblotting in shCont, shBMK1 or shCont and shBMK1 A549 cells transfected with DEPTOR. Protein expression level in EV or shCont cells was set at 1.0. (E) Schematic representation of the molecular mechanism by which BMK1 suppresses EMT. (F) Expression levels of E-cadherin, DEPTOR, and BMK1, as well as the phosphorylation state of Akt, in shCont and shBMK1 cell lines were examined by immunoblotting. ERK1/2 was used as a loading control. Protein expression level in shCont cells was set at 1.0.

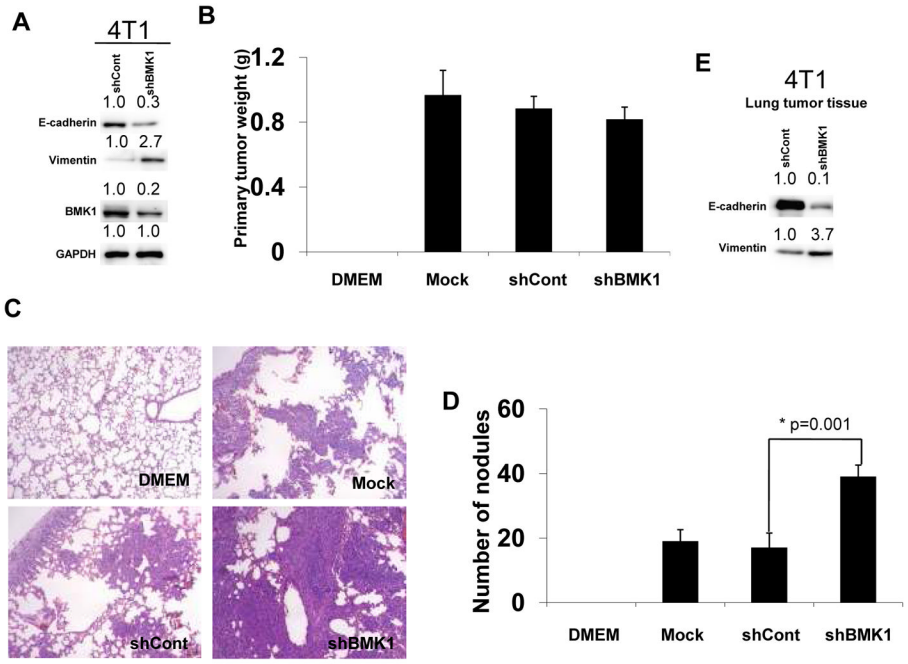


**Figure 5.**

BMK1 depletion promotes tumor metastasis in vivo

(A) 4T1 cells were infected with recombinant lentiviruses encoding shRNA against BMK1 (shBMK1) or with control virus (shCont). Expression levels of epithelial marker, E-cadherin, as well as mesenchymal marker, Vimentin, were examined by immunoblotting in shCont and shBMK1 4T1 cells. BMK1 expression was detected with anti-BMK1 antibody. Protein expression level in shCont cells was set at 1.0. (B) The weight of primary tumors formed by Mock, shCont and shBMK1 cells 3 week post-transplantation. (C) Lungs from mice injected with shBMK1, shCont 4T1, or parental 4T1 (Mock) cells were isolated and stained with H&E to determine cancer metastasis. (D) The number of lung surface metastases formed by Mock, shCont and shBMK1 cells 3 week post-transplantation. Error bars represent ±SEM. (E) Expression levels of epithelial marker, E-cadherin, as well as mesenchymal marker, Vimentin, were examined by immunoblotting in shCont and shBMK1 4T1 lung tumor tissues.